Green synthesis of ZnO nanoparticles and biological applications as broad-spectrum bactericidal, antibiofilm effects and biocompatibility studies on Zebrafish embryo

Iffat nasim[1], Chinnasamy Ragavendran[2]#, Chinnaperumal Kamaraj[3], Hayfa Habes Almutairi[4], Mir Waqas Alam[5], Kumar Manimaran[6], Ismini Nakouti[7]

[1]Department of Conservative Dentistry and Endodontics, Saveetha Dental College, Saveetha Institute of Medical and Technical Sciences (SIMATS), Saveetha University, Chennai-600 077, India, iffatnasim@saveetha.com

[2]Department of Cariology, Saveetha Dental College and Hospitals, Saveetha Institute of Medical and Technical Sciences (SIMATS), Saveetha University, Chennai-600 077, India, ragavan889@gmail.com

[3]Interdisciplinary Institute of Indian System of Medicine, SRM Institute of Science and Technology, SRM Nager, Kattankulathur – 603 203, Chengalpattu District, Tamil Nadu, India mullaikamaraj@gmail.com

[4]Department of Chemistry, College of Science, King Faisal University, Al-Ahsa 31982, Saudi Arabia. E.mail: halmutairi@kfu.edu.sa

[5]Department of Physics, College of Science, King Faisal University, Al-Ahsa 31982, Saudi Arabia; E. mail: wmir@kfu.edu.sa

[6]Research Center for Applied Microbiology, National Research and Innovation Agency (BRIN), JI. Raya Bogor KM. 46, Cibinong, 16911, Republic of Indonesia, manimaranbot@gmail.com.

[7]Centre for Natural Products Discovery (CNPD), School of Pharmacy and Biomolecular Sciences, Liverpool John Moores University, Liverpool L3 3AF, UK E. mail: I.Nakouti@ljmu.ac.uk

#Corresponding author:

Chinnasamy Ragavendran, Department of Cariology, Saveetha Dental College and Hospitals, Saveetha Institute of Medical and Technical Sciences (SIMATS), Saveetha University, Chennai-600 077, India. **E. mail**: ragavan889@gmail.com.

Abstract

This work generated zinc oxide nanoparticles (ZnO NPs) using *Ocimum tenuiflorum* in an inexpensive and environmentally friendly manner. The generated ZnO NPs were analysed using Ultra visible spectroscopy (UV-Vis), Fourier transformed infrared spectroscopy (FTIR), Scanning electron microscopy-Energy X-ray diffraction spectroscopy (SEM-EDX), Transmission electron microscopy (TEM), and X-ray diffraction (XRD). Bio-synthesized ZnO NPs showed UV–Visible absorbance maxima at 290 nm, indicating bio reduction and stability. The DRS spectra revealed a straight band gap value of 3.24 eV. Alcohols, alkanes, phenols, and amines in FTIR may contain reduced and capped zinc ions. Crystalline ZnO nanoparticles were verified by XRD. Biosynthesized ZnO NPs were exhibited in spherical and 5–35.49 nm in size by FESEM and TEM. EDX confirmed NPs zinc elemental signatures. Antibacterial properties showed that ZnO NPs effectively inhibited gram (+ve) and gram (-ve) pathogens, including *E. coli* (20.0±0.8mm), *E. faecalis* (20.0±0.5mm), *S. aureus* (18.01±1.2mm), and S. mutans (17.5±1.0mm). This study shows that biosynthesized ZnO NPs inhibit biofilm growth by 0.198-1.431 O.D values (Optical density). Antibiofilm inhibition was concentration-dependent. Nanoparticles proved effective against *E. coli*, *S. mutans*, *S. aureus*, and *E. faecalis* with MICs of 15 and 25 µg/mL. Time-dependent death kinetic studies indicated that 8-12 h ZnO NPs killed all bacteria. Also, ZnO NPs had low harmful effects on zebrafish eggs at doses upto 1mg/mL. In summary, the production of green ZnO NPs offers a sustainable and biocompatible approach that is well-suited for various biological applications.

Keywords: Green synthesis, ZnO NPs, Broad spectrum bactericidal properties, Antibiofilm, Zebrafish embryo

Graphical abstract

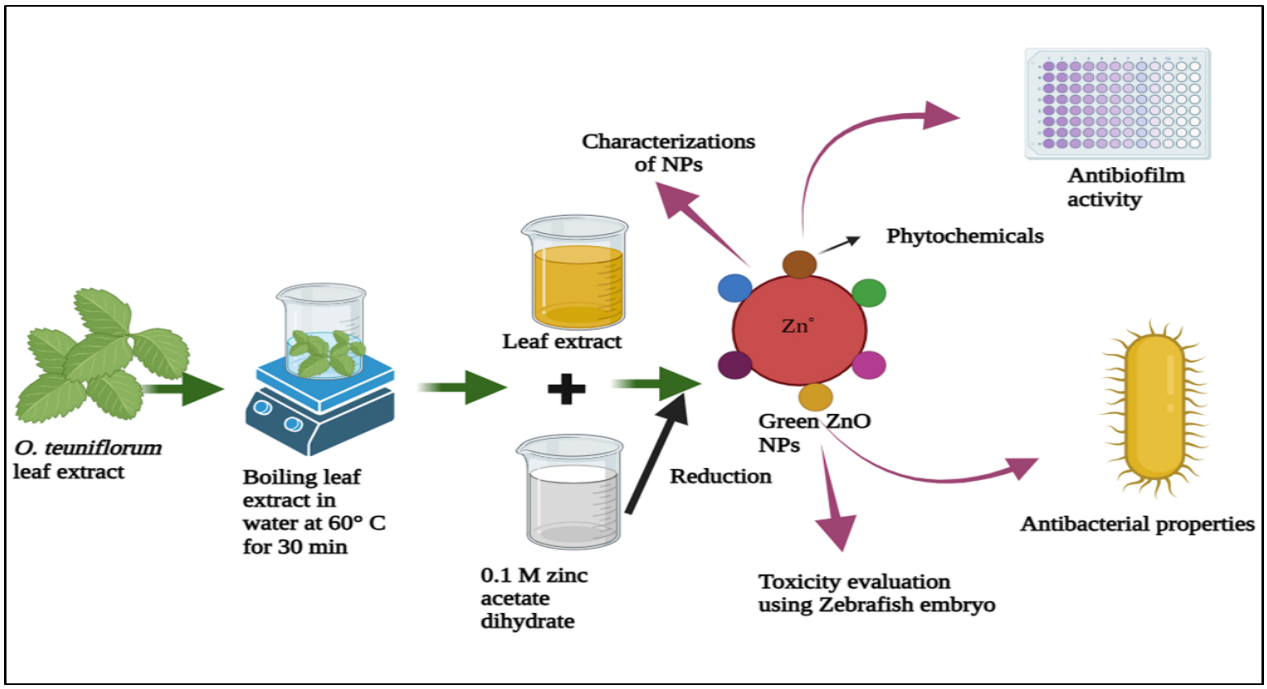

Introduction

Nanotechnology has recently been shown as a rapidly growing area. Many potential applications for nanoparticles (NPs) have been described in the fields of physics, chemistry, biology, electronics, antimicrobials, and agriculture [1]. Metallic nanomaterials advantages of being small and having a large surface area for interactions have drawn increased attention [2]. Various methods were employed for making nanomaterials of noble metals [3]. Traditional chemical processes involved the use of toxic chemicals, while greenly generated nanoparticles require less[4]. The usage of NPs of Nobel metals including gold, platinum, and zinc oxide in industrial and healthcare products is conventional in addition to catalysts [5]. However, the known chemical processes for producing nanoparticles are frequently costly, require hazardous chemicals, take a long time, and are prohibitively expensive. Therefore, there is a need for rapid, easy, affordable, and time-saving methods to create nanoparticles [6]. For the green synthesis of NPs utilizing different botanical extracts, various metal oxides, such as oxides of Ag, Cu, Au, etc., have been widely employed [7] [8].

Zinc oxide nanoparticles (ZnO NPs) have attracted increased attention in biomedical applications because it is occurrence in each cell of the human body and is crucial for the immune system. Although ZnO NPs are mostly utilized in the rubber sector for wear-proofing rubber composite, they may also be used to improve the polymers durability, intensity, antiaging, etc. features [9] [10]. ZnO NPs, serve a purpose in a multitude of industrial and personal care products. Its specific antibacterial and anticancer abilities have contributed to an increase in their uses within the biomedical industry [11][12]. Improvements in nanotechnology are not very important because of how they influence human health; therefore, for nanotechnology to be recognized interesting, green chemistry must be combined with nanotechnology [13]; [14]. In nanotechnology and materials research, the production of nanoparticles, particularly zinc oxide nanoparticles, is frequently achieved by the ecologically safe utilization of plant extracts such as *Ocimum tenuiflorum*. Because these plant extracts include reducing agents and bioactive chemicals that can help reduce metal ions and create nanoparticles, they are employed [15]. Sustainable production of metallic nanoparticles, specifically employing different plant parts including leaf, root, seed, and fruit pulp as a reducing and capping agent, is emphasized to alleviate concerns regarding the adverse effects of nanoparticles in medicinal and technical applications [16][17]. Vegetable varieties are one of the most often employed materials during the process of green synthesis. Terpenes, polyphenols, carbohydrates, alkaloids, and proteins are a few plant metabolites that are crucial for the production of NPs [18][19].

Dental caries is a common health problem that affects people of all ages[20]. It is mostly brought on by the bacteria *Streptococcus mutans* and *S. sobrinus*, which create acid and extracellular glucans that cause tooth decay[21] [22]. These bacteria produce biofilms, which function as barriers between them and the immune system and antibiotics, leading to illness and treatment resistance[23] [24]. There are serious health dangers associated with the emergence of Gram-positive and Gram-negative bacteria that are resistant to drugs, particularly for those with weakened immune systems[25] [26]. The creation of metal oxide nanoparticles with particular antibacterial qualities has been made possible by advancements in nanotechnology, providing a potential defence against these resistant microbes[27] [28] [29]. Combating dental caries requires the development of innovative strategies with improved antibacterial activity and fewer adverse effects[30] [31]. Promising substitutes for synthetic medications, plant-based products provide safer solutions for use by humans and animals alike[32]. Compared to synthetic medicines, herbal remedies made from medicinal

plants, like *Ocimum* species, are less toxic[32]. *Ocimum tenuiflorum*, popularly referred to as "Tulsi," is abundant in anthocyanins, flavonoids, and phenolic compounds[33]. *O. tenuiflorum* is a native of tropical and semitropical countries in Africa, Asia, and the Americas[34]. It is used extensively in medicine to treat bacterial infections, headaches, kidney diseases, and other conditions[35]; [36].. Its leaves, seeds, and essential oils are widely used in meals, cosmetics, and soaps[37]. It is grown professionally for usage in the cosmetic and pharmaceutical industries, as well as to flavour dishes including drinks, salads, and candies[38]. Studies have demonstrated the antimicrobial, antiviral, antioxidant, and anti-inflammatory properties of holy basil, which are ascribed to its phytochemical constituents, specifically the terpenoids and phenylpropanoids found in its essential oils[39] [40]. Among these, methyl eugenol and eugenol are important volatile chemicals with antioxidant, antiseptic, antimicrobial, and antifungal qualities[41] [42]. Research has shown that eugenol-containing essential oils have antibacterial properties against both Gram +ve and Gram-ve bacteria, with Gram +ve bacteria showing more sensitivity to these effects[43].

Zebrafish (*Danio rerio*) embryos are good and highly efficient *in vivo* models for evaluating of toxic substances in the environment including NPs [44]. The detrimental properties and processes of exposure to various amounts of AgNPs were recently investigated in research that we just published [45]. The present study used a zebrafish embryo system. Zebrafish are an ideal choice for a vertebrate prototype because of their high reproduction rate, affordable prices, visible transparency, and large number of transgenic animals that are easily accessible [46]. The use of embryos in zebrafish for evaluation of acute, early-life, and sublethal toxicological markers for developmental toxicities represents a promising option [47]. The objectives of this study were to: (i) produce ZnO NPs in a sustainable manner using leaf extract from *Ocimum tenuiflorum*; (ii) evaluate the antibacterial properties of ZnO NPs against gram-positive bacteria that cause dental caries, which is a novel contribution; and (iii) develop a sustainable, affordable synthesis process for testing antibiofilm and time-killing kinetic activity. The FTIR, SEM-TEM, EDAX, and XRD approaches were used to characterize the ZnO NPs.

Materials and Methods

Chemicals and reagents

The supplier of the precursor zinc nitrate hexahydrate $(NO_3)_2 \bullet 6H_2O$), Sigma Aldrich chemicals Pvt. Ltd. (India), provided 99% pure, (M.W: 297.48). Hi-Media, India provided

Mueller Hinton Agar, sodium hydroxide (NaOH), Whatman filter paper (WHA10348903), phosphate buffered saline (PBS) tablets (pH 7.4), and crystal violet (c3886). Throughout the investigation, freshly developed double-distilled deionized water was used.

Collection and preparation of plant materials

Ocimum tenuiflorum leaves were collected in the Guttoor Village, Dodda Belur (Post) Krishnagiri District of Tamil Nadu, India. The collected *O. tenuiflorum* leaves were carefully washed in tap water to get free of all the dirt and debris. Dried leaves have been chopped into a fine powder to produce the form of powdered material. 10 g of the dry powder was boiled in 100 mL of water for 30 min in room temperature. The mixture was filtered by Whatmann No. 1 filter paper to yield the water-based leaves extract after 2 h. The aqueous extract was cooled to 4 ºC in a refrigerated prior it was utilized for producing ZnO NPs [48].

Green synthesis of ZnO NPs

About 0.1 M zinc acetate hexahydrate has been mixed in 80 mL of milli-Q water and dissolved for 15 min at room temperature with continuous stirring. Then, 20 mL of an aqueous leaf extract liquid was mixed with the zinc acetate solution. The resulting mixture was rapidly stirred for 2 h at 70 °C using magnetic stirrer. The resulting precipitate was allowed to cool down when the reaction was finished, and it was successful. Centrifugal force was used for separating the resulting product from the reaction solution for 15 min at 12000 rpm. Those residual particles were washed in deionized water in subsequent steps, and then the items were dehydrated in a hot air oven at 80 °C. After synthesized, the NPs was heated in a muffle chamber for 2 h at 400°C. Following drying out, the ZnO NPs were crushed and stored in an Eppendorf tube [49].

Characterization of ZnO NPs

The first approach in synthesizing NPs is recognizing their structure, characteristics, and response mechanism. To identify this, several methods of categorizing have been employed. The UV–Visible absorption spectrum of the synthesized ZnO-NPs was detected using a Shimadzu UV-1601 UV–visible spectrophotometer [50]. To measure the crystalline structure of ZnO NPs, the material was analyzed using a Brucker X-ray diffractometer (XRD-6000) with Cu-Ka energy as a source of X-rays having a spectrum of K = 1.541 Aº [51]. Using a Bruker alpha-P FTIR spectrum analyzer calibrated to run between 4000 and 400 cm^{-1}, the functional groups found in the leaf extract were determined [52]. The ZnO NPs were coated to an aluminum sample holder with conductive carbon tape for SEM examination. We

employed a JEOL field emission electron microscope, model JSM7800F, with an OXFORD microprobe for analysis of EDS with a wavelength of 0.7 nm. The shape and structure of the nanomaterials were identified employing a transmission electron microscope (TEM) equipped with a LaB 6 electron cannon and a 30 kV voltage to accelerate at room temperature [53].

Antibacterial properties of ZnO NPs

Four human pathogenic bacterial strains such as *Staphylococcus aureus* (ATCC-25923), *Escherichia coli* (ATCC-25922), *Streptococcus mutans* (MTCC-890), and *Enterococcus faecalis* collected from the Saveetha Dental College and Hospitals were examined for the produced ZnO NPs antibacterial property [54]. The Mueller Hinton agar (MHA) medium was used for maintaining bacterial strains, and the well diffusion approach was used to measure antibiotic activity on MH agar plates. Nutrient agar was autoclaved at 121°C for 15 min. Prepared nutrient medium (20 mL) was then pour into each sterile Petri plate and allowed to cool down in the aseptic environment in the laminar airflow hood. The test microorganisms from the overnight-grown (0.1 mL contains 0.5 McFarland suspensions at 10^7 CFU/mL) inoculation broth culture was distributed equally using sterile cotton swabs. The agar was punctured to make 5 mm-diameter wells. ZnO NPs that were bio-fabricated were administered to the bacterial strains at concentration of 50 and 100 µg/mL overnight. For each petri dish, a cefotaxime reference drug (5 µg/mL) was utilized as a positive control, while a negative control was 10% dimethyl sulphoxide (DMSO) (50 µl/well, v/v). The plates were then kept at 37º C for 24 h in a bacteriological incubator. Each test was done three times and the average inhibition zone value for a specific dose was calculated to determine results.

Minimum inhibitory concentration (MIC)

The minimal inhibitory concentrations (MICs) of ZnO NPs were measured using broth microdilution in 96-well microtiter plates. The results were obtained following CLSI (2012) standards with some modifications [55]. After 0.1 mL of nanoparticle suspensions were added to each well, which had already received 0.1 mL of Mueller Hinton broth media, the concentrations were split by two to get final values of 0.5, 1, 2.5, 5, 7.5, 10, 12.5, 15, 25, 50, 100, and 200 µg/mL. Then, each well received 50 µL of normal inoculum. 24 h after being incubated at 37 °C. The optical density (O.D.) of microbial growth was measured at 600 nm. The MIC endpoint was defined as the lowest concentration of ZnO NPs at which no microbial growth was observed after incubation. As a positive control (cefotaxime), bacteria-inoculated media was employed. The only negative controls employed are 10% DMSO.

Killing kinetic assay

The killing kinetic test was performed to detect the rate at which ZnO NPs inhibited the growth of bacterial cultures [56]. Three separate bacterial strains were cultured overnight, and the next day, 5 µL (10^6 CFU/mL) of their development was transferred into tubes containing 1 mL of broth before being exposed to the proper MIC doses of ZnO NPs. Bacterial viability was determined at 0, 2, 4, 6, 8, 10 and 12 h and compared to a positive control (cefotaxime-no treatment). With nutritional broth used as a reference, an assessment was carried out using a spectrophotometer at 600 nm.

***In vitro* antibiofilm assessment assay**

The 96-well microtiter plate approach was used for evaluating the efficiency of ZnO NPs in biofilm formation [57]. To each well of the sterile microtiter plate, 180 µL of MH broth was added, and 10 µL of an overnight-grown culture was introduced as the inoculum. ZnO NPs and antibiotic (positive control- cefotaxime 5 µg/mL) have been added to the solution at different amounts ranging from 20 to 100 µg/mL. The wells were then maintained for 24 h at 37ºC in bacteriological incubator. Following incubation, each well components were carefully transferred to other wells. After being cleaned with 200 µL of sterile distilled water, the tubes were dried for 5 min. Following the addition, 0.2% (w/v) crystal violet was incubated for 30 min at 37ºC. After discarding the crystal violet, it was left to air-dry. A solution of 95% ethanol has been added following drying, and a spectrophotometer was utilized to determine the absorbance at OD (optical density) 595 nm. These OD values were used as an indicator for the degree to which bacteria attached to surfaces and developed biofilms. Each test was performed in triplicate and three times.

Maintenance of Zebrafish

Wild AB zebrafish (*Danio rerio*) were collected from Raj Fish Aquarium in Chennai, Tamil Nadu, and developed in a circulating culture technique. Aquaria containing sieved tap water with an oxygen content of higher than 80% and a pH of 7.0±0.3 were home to females and males at the age of 6 to 12 months, who were maintained in a percentage of 2:1. The water was kept at a constant 26 °C using a 14 h: 10 h day and night schedule. Zebrafish were consistently supplied an extensive diet that included newly hatched live brine shrimp (*Artemia* nauplii) once daily in the pre-lunch, as well as once daily in the evening, vitamin-fed powdered flake meal.

Embryo collection and acute toxicity assessment

Male to female zebrafish were kept in reproductive boxes in a ratio of 1:2 after being chosen as sexually mature. A glass barrier was used to separate the men and females, and the fish and demersal eggs were divided before the light was turned off by holding the titanium mesh vertically 5 cm above the bottom of the container. The male and female fish engaged the next day, and eggs were deposited when the clapboard was removed. The fertilized embryos were recovered after around 30 minutes. To get rid of the contaminants, the embryos were washed twice or three times using water produced in accordance with ISO 15088 standard. To evaluate for toxicity, the 2-4 cell phase embryos were chosen and cultivated for 2-4 hours post-fertilization (hpf). 90% fertilization rate was established as the minimal standard for processing additional studies [58].

Zebrafish embryos were exposed to an acute toxicity test in accordance with OECD 236 and other conventional and significantly modified standardized aquatic methods (ARRIVE guidelines- [59]. Twenty embryos were placed in each well of 6-well cell plates used for exposure tests. Assay mixtures were developed using dissolved stocks (5 mg/mL) of *O. teuniflorum* synthesized ZnO NPs that had been produced. The magnetic stirrer was regularly examined to sustain the suspension while preparing the dilutions. Different ZnO NPs concentrations, including control, 250, 500, 750 µg/mL, and 1 mg/mL with water worked as a control group in this investigation, and were employed in the experiment, which was then incubated at (27±1) °C started at 4 hpf with a light/dark ratio of 14/10 h. Each test was carried out three times. Toxicology was assessed using embryo/larval survival and embryo hatching rates [60]. Every 24 h, the exposure medium was replaced, and the deceased embryos were immediately removed. At 24, 48, 72, and 96 hpf, malformed embryos were identified. Under the Leica M205C stereomicroscope (Leica Microsystems, Inc.), representative abnormal zebrafish embryos were chosen and captured on camera. The number of malformed and hatched embryos was counted, and the rate of malformation and hatched embryos was computed [61].

Data analysis

Results are presented as Mean ±SD. The statistical evaluation was carried out using GraphPad Prism 8 software and the student-t test or one-way analyses of variance (ANOVA), as applicable. Results were considered statistically significant at $p< 0.05$.

Results and Discussion

Characterization of NPs

Plant-mediated vibrant nanoparticle production is more rapid and greener than existing approaches. Zinc nanoparticles are a promising alternative to antibiotics due to their antibacterial capabilities and new bioactive chemicals [62]. *O. teuniflorum* leaf extract can have phytoconstituents to cure different ailments. Alkaloids, flavonoids, steroids, phenols, glycosides, and terpenoids are found in aerial portions[63]. The soluble substances in *O. teuniflorum* leaf aqueous extract might reduce metal ions and stabilize NPs. Based on previous phytochemical investigations [64], the plant is an excellent source of reducing carbohydrates, polyphenols, eugenol, flavonoids, carvacrol, minerals, ocimene, oleanolic acid, ursolic acid, rosmarinic acid, eugenol, and linalool. These compounds have the ability to maintain stability and interact nanoparticles; Supplementary Fig.1. illustrates the probable route of synthesis for ZnO NPs. The stimulation of surface plasmon resonance of nanomaterials induced the appearance of the water-based extract changing from dark brown to bright yellow resulting from exposure with zinc acetate solution (**Fig**. 1**A**). To find the absorption peak of the bio-synthesized ZnO NPs, a UV/Vis spectrophotometer measurement was carried out within the spectral between 250 to 500 nm. Zinc oxide nanoparticles demonstrated an evident single peak with the highest absorption wavelength at 290 nm (**Fig. 1B**). There are significant distinctions between the excited electronic configurations of pure ZnO and superconducting ZnO NPs exhibiting a direct energy band gap of 3.24 eV. In ZnO NPs, this change leads to a quantum confinement phenomenon. In the ultraviolet, the ZnO particle showed signs of intrinsic absorption peaks. Band gaps were computed using the formula $\alpha = A (h\nu \pi - Eg)^n / h\nu$, where α is the absorption coefficient, as illustrated in Fig. 2C [65]. Because of ZnO energy band gap, there may be higher light absorption during the ultraviolet, which could promote the formation of more eπ - h+ pairs and increase antibacterial efficacy. The intensity of nanoparticle absorption peak in UV–visible spectrum is linked to particle size. Similarly, [66] investigated the phyto-mediated production of ZnO NPs of *Berberis aristata* with a 343 nm UV spectrum.

FTIR analysis of biosynthesized ZnO NPs

FTIR examination is an excellent method for chemical detection because every molecule or chemical structure has a specific spectrum pattern. **Fig.2** demonstrates many major and minor stabilized ZnO nanoparticle FTIR spectra of *O. teuniflorum* leaf extract (3314, 2915, 2845, 1616, 1027 cm^{-1}) and the biosynthesized ZnO NPs at 3574, 3322, 2915, 1360, and 753 cm^{-1} were absorption bands (**Table 1**). The leaf extract lacks a few bands (3574 cm^{-1}) compared with produced ZnO NPs, and the bands shift indicates few functional molecules play a role in

the reduction mechanism. FT-IR spectrum between 3574 to 3314 cm^{-1} demonstrate alcohol and phenol bands due to O-H stretching vibration. Based to investigations earlier achieved by [67]; [68] hydroxyl groups (O-H) have more potential for associating with zinc ions than other kinds of groups. The O-H stretching vibration, or 3477 cm^{-1} band, is generally linked to ZnO nanoparticles and indicates the presence of hydroxyl groups (-OH) on their surface. These hydroxyl groups may come from surface hydroxylation during synthesis, or they may come from leftover water molecules adsorbed on the surface of the nanoparticle. Furthermore, during the creation of ZnO NPs, the hydroxyl groups can take part in the bio-reduction process. A unique pattern at wavenumber 3574 cm^{-1} reveals the O-H stretching vibration of alcohol and phenol hydroxyl groups. Absorption bands at 2915 cm^{-1} are due to C-H stretching of the aromatic groups. The medium absorption band at 2845 cm^{-1} is due to the stretching vibrations of alkanes (C-H). C-H bond bending vibrations or C-O stretching vibrations may be responsible for the band at 1360 cm^{-1} (C-H bending or C-O stretching). This band is present in the ZnO nanoparticles spectrum, but it is absent from the extract, suggesting that the ZnO nanoparticles surface now contains new organic residues. These residues are most likely the result of the extract's organic molecules breaking down or of stabilizing agents being used during the process of synthesis. The band at 1675 cm^{-1} could be attributed to -C=C- stretching vibrations of alkene groups. The band at 1616 cm^{-1} may be linked to the N-H groups of polyols in the material, which include flavanones, terpenoids, and carbohydrates. On the other hand, the band shift from 1027 cm^{-1} corresponds to the binding of the C–N aliphatic amine group associated with the reduction of nanoparticles [69]. The band recorded at 753 cm^{-1} could be assigned to C-H bending, Zn-O groups. Zn-O bonds interact at a range of 400–800 cm^{-1}. This indicates that the ZnO bonds are clearly represented by 404 and 702 cm^{-1}.Water-based leaf extract polyols oxidize aliphatic and primary amine molecules to minimize metallic ions [70]. In the present study, *O. teuniflorum* leaf extract contains phenols, alcohols, carboxylic acids, and alkanes bind to ZnO NPs, whereas phenols and alcohols attached stronger, which may have served as stabilizing and reducing substances towards the synthesis of ZnO NPs [71]. FTIR spectrum analysis confirmed the XRD outcomes and shown no additional impurity particles. The bands in the 400-800 cm^{-1} band link to stretching and bending of ZnO that results from the interaction of ZnO NPs with carbonyl groups, leading to a coating layer over the ZnO NPs surface that inhibits aggregation and agglomeration, as previously stated [72].

XRD study of ZnO NPs

XRD proves ZnO NPs crystalline structure. The diffractogram shows wave intensity versus diffraction angle. XRD confirmed crystalline *O. teuniflorum* produced ZnO NPs (**Fig.3**). The ZnO NPs diffraction peak values at (100), (002), (101), (102), (110), and (103) are depicted in the figure. These correspond, in turn, to the degrees (2θ) at 31.34°, 34.50°, 36.32°, 47.60°, 56.68°, and 62.94° which is corresponds to JCPDS:36-1451. Elevated diffraction peaks signified the crystalline structure of the material. There were no peaks identified because of impurities, and the peaks strength outlines were a property of the nanoparticle's spherical wurtzite structure. Scherrer's formula estimated a 10–25 nm crystallite size. Our results are similar to [73], who generated zinc nanoparticles using *O. americanum* leaf extract, and [74], who used *O. sanctum* leaf extract. ZnO NPs with boosted antibacterial features may have additional diffraction peaks (32.24°, 57.5° and 74.58°) that arise due to the binding of antibacterial agents to their surface[75]. Diffraction study demonstrated that antagonistic bacteria antibacterial compounds may react with Zn $(NO_3)_2$ solution to produce ZnO NPs, which surface adsorbed various antibacterial molecules [76].

FESEM, EDAX and TEM analysis

The images obtained from FESEM were obtained at various levels of magnification to evaluate the form and dimension of the produced nanoparticles, as shown in **Fig.4** Surface texture confirms nanoparticle aggregation. ZnO synergistic effect is affected by surface morphology [77]. XRD stated the particles were predominantly spherical. EDX also proves highly useful because it supports the chemical characterization or elemental evaluation of a material [78]. The EDX spectrum (Supplementary Fig. 2) showed zinc (Zn) and oxygen (O), confirming ZnO NP production. EDX displays significant peaks of 68.11% for Zinc and 31.89% for Oxygen, whose weight% peaks are very close to those reported before for ZnO nanoparticle production (Pai et al., 2019). Zinc has two high peaks at 1eV and 8.6 eV, and Oxygen had one at 0.3 eV. The compound's elemental makeup is confirmed by these Zinc and Oxygen measurements [79]. Finally, ZnO NP morphological structures were examined by TEM (JEOL JEM-1220). TEM image and particle histogram of *O. teuniflorum* leaf extract-synthesized ZnO NPs are shown in **Fig.4** TEM pictures exhibited produced nanoparticles at various magnifications are displayed in **Fig. 4C, D &E**. Median 5–35 nm, *O. teuniflorum* fabricated ZnO NPs were 29 nm spherical. The TEM data confirmed some region aggregation of ZnO NPs. Similarly, Aggarwal et al. (2023) reported hexagonal ZnO NPs biosynthesized from *Ocimum basilicum* leaf extract with a median particle size (20 nm). The characterisation method determined the dimension and crystal structure of ZnO NPs, leading

to their use in application research. The structure of NPs determines efficacy against infections [80]. Because spherical NPs quickly penetrate pathogen cell walls, their antibacterial effect is potent [81]. ZnO NPs made from *O. teuniflorum* extract can cure infections in humans well.

Antibacterial properties of ZnO NPs

The cell envelope and membrane components of Gram-positive and Gram-negative bacteria are different which must be taken consideration when synthesizing successful functionalized metallic nanoparticles. Bactericidal properties are exhibited by metallic nanoparticles that enter the bacterial cell wall. Therefore, once intracellular biological functions are interrupted by nanoparticles, the result is apoptosis, or the death of microorganisms. The prevention of DNA replication, protein leakage, mitochondrial failure, protein damage, membrane rupture, or direct entrance of NPs via the cell wall, and breakdown in the electron transport chain are these key mechanisms of the antimicrobial mechanism [82]. The potential of synthesized ZnO NPs formed by *O. tenuiflorum* to inhibit four distinct human pathogenic bacteria was investigated. ZnO NPs synthesized by *O. tenuiflorum* exhibited significant antibacterial efficacy against all evaluated bacterial strains. Diameter of each well is 5 mm. At a concentration of 100 µg/mL, it was determined that biosynthesized ZnO NPs had the excellent antibacterial effects against *E. coli* (20.05±0.8mm), *E. faecalis* (20.0±0.5mm), *S. aureus* (18.01±1.2mm), and *S. mutans* (17.5±1.0mm) Supplementary Fig.3. The dimension of the zone of inhibition was used to calculate antibacterial properties against pathogenic microorganisms (**Fig.5)**. This study found that ZnO NPs were more efficient against gram (-ve) bacteria than gram (+ve) bacteria [83]. Interesting that *Punica granatum* extract-made ZnO NPs (4–10 nm) inhibited pathogenic microbe growth better than bigger sizes [84]. Yang et al. [85] study examined the effectiveness of ZnO NPs utilizing leaves from the *Hibiscus cannabinum* plant, which demonstrated significant efficacy against the microorganisms *E. coli* and *S. aureus*. Gram (+ve) bacteria have a rich peptidoglycan layer and no outer lipid membrane. Gram (-ve) bacteria have an exterior lipid barrier and a thin peptidoglycan surface. Nanoparticles have distinct attachment strategies due to cell wall differences. ZnO NPs stick to cell walls and membranes, affecting structural integrity, transport, and porosity [86]. ZnO NPs are more effective against Gram (-ve) bacteria due to their weaker cell walls and thinner peptidoglycan covers. NPs bind to Gram (-ve) bacteria Lipopolysaccharide due to their negative electrical charge [87]. The bacteria-ZnO NPs interaction involves ZnO NPs

adherence to the bacterial cell wall [88]. ZnO is considered a safe metal oxide due to its high toxicity towards bacteria and low toxicity against eukaryotic cells [89].

Determination of minimal inhibitory concentration

The bactericidal capacity of green synthesized ZnO NPs was examined by comparing the MIC rate against human pathogenic oral and clinical bacteria to the conventional antibiotic sensitivity. The outcomes of the present study strongly exhibited that four tested strains of bacteria might be reduced in density by treatment with *O. tenuiflorum*-fabricated ZnO NPs via a concentration-mediated approach. The initially detected ZnO NP doses that inhibited the growth of the chosen bacterial strains were recorded as a particular MIC value. MIC is the minimum inhibitory concentration of an antibacterial agent that totally inhibits bacterial growth. The *E. coli* strains minimum inhibitory concentration (MIC) was found to be 25 µg/mL, whereas the positive control (cefotaxime) showed 2.5 µg/mL (Supplementary Fig.4A), but the *S. aureus* bacterial strain revealed a MIC value of 15 µg/mL and positive control inhibited 5 µg/mL (Supplementary Fig.4B), followed by the MIC values of 15 µg/ mL for *S. mutans,* whereas positive control inhibited 10 µg/mL (Supplementary Fig.4C) and 25 µg/ mL for *E. faecalis*, whereas cefotaxime (positive control) inhibited 12 µg/mL (Supplementary Fig.4D). Based on the findings, it was observed that the green derived ZnO NPs demonstrated a minimum inhibitory concentration (MIC) ranging from 2.5 µg/mL to 12 µg/mL for each pathogen examined, suggesting that the synthesized ZnO NPs effectively inhibited the growth of these pathogens. The 2019 CLSI guideline determined antimicrobial susceptibility categories, or MIC breakpoints. The positively charged Zn+ ions in ZnO NPs interacted to the bacterial cell membrane in the present study. This connection established an electrical communicate with the negatively charged cell wall and plasma membrane, disrupting it [90] [91]. The present research found that compared to *S. aureus* and *S. mutans* strains, *E. coli* and *E. faecalis* bacteria had significantly higher MIC values. This may be driven on by the peptidoglycan layers as well as structural changes in the cell membrane [92].

Time killing kinetic assay of pathogenic strains

A bacteria-killing rate study determines the length of time ZnO NPs require to eradicate bacterial strains. The killing kinetic graph demonstrated that produced ZnO NPs consistently reduced *E. coli*, *S. aureus*, *S. mutans*, and *E. faecalis* growth. All four bacterial strains inhibited growth significantly between 8 or 10 h of exposure to their MIC dosage and nanoparticle concentration (Fig.6). This reduction was dependent on time and ZnO NPs concentrations. It's probably due to ZnO NPs intracellular penetration after enough time.

After 12 h, bacteria exposed to ZnO NPs at their MIC quantities for more time than the positive control died. The dose-dependent time-killing property of ZnO NPs against human pathogenic bacterial strains was similarly reported by Ifeanyichukwu et al. [93]. Likewise, Hayat et al. [94] investigated the time-killing assay of *Acacia arabica*-biosynthesized ZnO NPs tested against *S. aureus* and *E. coli*. Zn^{+} ion binding to the bacterial cell skin denatures the protein [90]. In summary, ZnO NPs demonstrated broad-spectrum efficacy against tested microorganisms. Green manufactured ZnO NPs are strong antibacterial agents because they kill human pathogenic microorganisms.

Evaluation of antibiofilm activity

Biofilms are composed of layers of polysaccharides, nucleic acids, sugars, and proteins on living or non-living surfaces. Strong biofilm layer concerns affect human health and environment in food business, wastewater management plant, and water supply network [95]. It is considered that the most frequent biofilm-forming bacterial strains, such as *E. coli*, *S. aureus*, *S. mutans*, and *E. faecalis*, cause approximately 60% of the infections [96]. (Supplementary Fig.5) shows the antibiofilm activity of *O. teuniflorum* produced ZnO NPs against biofilm-forming pathogens at 20-100µg/mL. ZnO NPs had O.D values 0.198 ± 0.21 to 0.845 ± 0.1 (O.D) antibiofilm activity against all tested pathogens at 20µg/mL. the antibiofilm activity of ZnO NPs against tested bacteria increased significantly ($p \leq 0.05$) and concentration-dependent. The maximum antibiofilm properties of *O. teuniflorum* synthesized ZnO NPs towards *E. coli*, *S. aureus*, *S. mutans*, and *E. faecalis* was 0.205 ± 0.2, 0.304 ± 0.1, 0.634 ± 0.2, and 0.845 ± 0.1% at 100µg/mL. Similarly, Fernandes et al., [97] reported the *Cystoseira* algae derived the silver and gold nanoparticles exhibited the inhibit the formation of biofilms using *Pseudomonas aeruginosa* and *S. aureus*. Unni et al., [98] reported *Piper longum* synthesized ZnO nanoparticles reduce biofilm development. The biofilm inhibition by fabricated nanoparticles was highest in *S. mutans*, followed by *S. aureus*, *E. coli* and lowest in *E. faecalis*. Zinc oxide nanoparticles dependent on dose inhibited *Bacillus* sp biofilm formation, according to [99]. Likewise, Altaf et al., [100] found that TiO_2-NPs made with *Carum copticum* extract effectively eliminated *E. coli*, *P. aeruginosa*, and *S. aureus* biofilms by 60.09, 64.14, and 48.30%, respectively. Zinc nanoparticles reduced biofilm development in [101]. ZnO NPs produced from *O. teuniflorum* aqueous extract reduce biofilm development of selected gram (+ve) and gram (-ve) bacteria. Notably, ZnO NPs shown strong antibiofilm properties against *S. aureus* [102]. At high concentrations, eco-

friendly ZnO NPs produced from *O. teuniflorum* reduced biofilm development without disrupting humans or the environment.

Biocompatibility studies on zebrafish embryo

Numerous investigations have shown the biocompatibility of metal and metal oxide NPs in zebrafish embryos [103]. Metal oxide NPs cytotoxicity in zebrafish embryos depends on their form, size, and surface area. Zebrafish embryos can be utilized for *in vivo* assays for preclinical drug discovery for human diseases. Zebrafish and humans have 85% genomic homology [104]. Zebrafish embryos were treated to ZnO NPs at 250–1mg/mL to assess ZnO NP toxic effects. The figure shows the no toxicity of untreated and (p> 0.05) effects at doses of 250 and 750 μg/mL, across all exposure periods. Increasing ZnO nanoparticle concentrations to 1mg/mL had a small impact (p< 0:001) on embryo mortality. A substantial increase in fish mortality (p< 0.05) was seen up to 96 hpf with increasing nanoparticle concentration. Using 1mg/mL of ZnO nanoparticles caused in 5% embryo death at 96 hpf (**Fig. 7A**). The hatching rate of zebrafish embryos is marginally changed by increasing ZnO nanoparticle dosage. The untreated embryos had a 100% hatch rate, whereas the 1mg/mL ZnO nanoparticle-treated embryos had a 90±1:7% hatch rate (**Fig.8A**). There were no significant variations in hatching percentages between 500 and 750 μg/mL ZnO nanoparticle groups. Concentrations of 500 and 750 μg/mL had p values below 0.01 (p < 0:01). The hatching rate was slightly significant (p< 0.05) and decreased with nanoparticle concentration up to 750 μg/mL (**Fig.8B**). While increasing ZnO NP concentration, **Fig.8B** indicates slight delayed hatching. Zebrafish tail bending and growth retardation were mild at higher ZnO nanoparticle concentrations. The control group without treatment zebrafish exhibits normal development and no delayed activity. The 750 μg/mL concentration did not cause any severe malfunctions or developmental toxicity up to 96 hpf. Exposure to ZnO nanoparticles over 1mg/mL produced axial and tail bends, pericardial edema, and decreased digestive tract in embryos. Based on produced ZnO NP concentrations, the body dimension was considerably lower than in untreated groups (**Fig.8E**). Similarly, Choi et al. [105] found that ZnO NPs administered to zebrafish embryos reduced body length compared with untreated groups. All tested groups exhibited far lower heartbeat counts than the "1 mg/mL" group (**Fig.8C**). Malformation caused by biosynthesized ZnO NPs was viewed in both the treated and untreated groups of embryos in the present study. Zebrafish embryos in control groups were malformation-free (**Fig.8D**). At 1mg/L, embryos had modest abnormalities as tail bending and pericardial edema (**Fig.7B**). This study confirms previous findings on the toxicity of ZnO

NPs and Zn ions on zebrafish embryos throughout the 96-hpf period [106] [107]. The current findings resulted in ZnO NP concentrations, although the body length was much smaller than in the control groups. Similarly, Lee et al., (2022) found that ZnO NPs treated zebrafish embryos had shorter bodies than untreated groups. The biogenic ZnO NPs was given to *Danio rerio* at a dose of 750 µg/mL without any negative effects. This research hopes to develop an efficient bioprocess for synthesizing zinc nanoparticles, which will be useful in therapeutic uses.

Conclusion

The present research attempted to synthesize nanoparticles and characterize them using tools such as UV, XRD, FTIR, SEM-EDX, and TEM. Additionally, research was done on the biological uses, including anti-bacterial, anti-biofilm, and biocompatibility investigations on zebrafish embryos. UV–visible wavelength spectrum analysis proved biosynthesized surface plasmon resonance. *O. teuniflorum* leaf extract synthesized ZnO NPs absorption spectra at UV wavelengths between 200 and 400 nm indicated maximum around 290 nm. A prominent peak was evident in the FTIR spectrum values at 3477.2 cm^{-1}, which is associated with the stretching of phenolic or alcoholic molecules by dimer -OH. The TEM pictures displayed ZnO NPs with spherical forms and diameters ranging from 5 to 35 nm. Biosynthesized ZnO NPs showed strong antibacterial and antibiofilm properties against tested dental/clinical pathogens. Moreover, ZnO NPs produced by *O. teuniflorum* having inhibitory zones shown strong antibacterial activity against bacteria that cause disease in humans. Maximum efficiency was achieved by *E. coli* (20.05±0.8mm) at 100 µg/mL. Gram (+ve) ZnO NPs have a significant antibacterial effect and prevent biofilm formation, with *S. aureus* and *S. mutans* showing the similar MIC value at 15 µg/mL and Gram (-ve) *E. coli* showing a distinct outcome (25 µg/mL). Time- and dose-dependent killing mode of ZnO NPs involves bacterial strain metabolic system penetration, resulting in cell death. These biosynthesized nanoparticles may offer an alternate therapy for multidrug-resistant bacteria. A zebrafish embryo was employed to test the toxicity of the nanoparticles. The hatching and survival rate of zebrafish embryos were not impacted by ZnO NPs aqueous solution concentrations of 750 µg/mL. The study suggests that ZnO NPs can effectively reduce dental caries-causing organisms without the need of synthetic antibiotics. The biosynthesized ZnO NPs may be a promising biological disease-controlling agent for oral infections. The findings of this investigation suggest that *O. teuniflorum* derived ZnO NPs have several significant applications in the pharmaceutical and biological domains.

Credit authorship contribution statement

CR conceived and designed the study, conducted experimental procedures, and, along with **IN, MWA &CK**, provided oversight and supervision for the study. **CR, CK & HHA** contributed scientific insights and participated in manuscript revision, provided oversight and supervision **CK** performed the embryotoxicity assessments, while **IN** contributed scientific insights and participated in manuscript revision, provided oversight and supervision **KM** contributed scientific insights and participated in manuscript revision. The article was reviewed and approved by each author.

Acknowledgements

This work was supported by the Deanship of Scientific Research, Vice Presidency for Graduate Studies and Scientific Research, King Faisal University, Saudi Arabia [Project No: KFU241610]. The authors would like to extend their heartfelt thanks to Saveetha Dental College and Hospitals, Saveetha Institute of Medical and Technical Sciences, and Saveetha University in Chennai, Tamil Nadu, India, for their continuous help in executing this investigation.

Funding

This research was supported by Researchers Supporting Project number Project No: KFU241610], King Faisal University, Saudi Arabia.

Conflict of Interests

Conflicts of interest are not reported.

Data Availability

The corresponding author can provide the current research's datasets upon reasonable request.

Declarations

Not Applicable

Ethical Approval

Not Applicable

Consent to Publish

576 Not Applicable

577 **Consent to Participate**

578 Not applicable.

579 **Competing Interests**

580

581 **References**

582 [1] C. Hano, B.H. Abbasi, Plant-based green synthesis of nanoparticles: Production,
583 characterization and applications, Biomolecules. 12 (2022).
584 https://doi.org/10.3390/biom12010031.

585 [2] Q. Yao, Z. Yu, L. Li, X. Huang, Strain and Surface Engineering of Multicomponent
586 Metallic Nanomaterials with Unconventional Phases, Chem. Rev. (2023).
587 https://doi.org/10.1021/acs.chemrev.3c00252.

588 [3] Y. Sharma, P. Kapoor, Noble metal nanostructures for various applications, Mater.
589 Today Proc. (2023). https://doi.org/10.1016/j.matpr.2023.03.628.

590 [4] N. Rani, P. Singh, S. Kumar, P. Kumar, V. Bhankar, K. Kumar, Plant-mediated
591 synthesis of nanoparticles and their applications: A review, Mater. Res. Bull. 163
592 (2023) 112233. https://doi.org/10.1016/j.materresbull.2023.112233.

593 [5] N.A.I. Md Ishak, S.K. Kamarudin, S.N. Timmiati, Green synthesis of metal and metal
594 oxide nanoparticles via plant extracts: an overview, Mater. Res. Express. 6 (2019).
595 https://doi.org/10.1088/2053-1591/ab4458.

596 [6] V. Manikandan, P. Velmurugan, J.-H. Park, W.-S. Chang, Y.-J. Park, P. Jayanthi, M.
597 Cho, B.-T. Oh, Green synthesis of silver oxide nanoparticles and its antibacterial
598 activity against dental pathogens, 3 Biotech. 7 (2017) 72.
599 https://doi.org/10.1007/s13205-017-0670-4.

600 [7] S. Dhir, R. Verma, S. Bhatt, V. Garg, R. Dutt, Green Synthesis, Characterization,
601 Biomed. Appl. Copp. Copp. Oxide Nanoparticles Plant Orig. 18 (2023) 391–406.

602 [8] R.P. Sharma, S.D. Shirsat, P. V. Shinde, S.S. Mohite, R.S. Mane, Nano-antimicrobial
603 Materials: Alternative Antimicrobial Approach, Nanomater. Sustain. Dev. (2023) 137–
604 171. https://doi.org/10.1007/978-981-99-1635-1_5.

[9] Z. Wang, Z. Hou, X. Liu, Z. Gu, H. Li, Q. Chen, Preparation of Zinc Oxide with Core–Shell Structure and Its Application in Rubber Products, Polymers (Basel). 15 (2023) 2353. https://doi.org/10.3390/polym15102353.

[10] N.B. Guerra, J. Bortoluz, A.R. Bystronski, A.E.D. Maddalozzo, D. Restelatto, M. Roesch-Ely, D.M. Devine, M. Giovanela, J.S. Crespo, Recent Progress on Natural Rubber-Based Materials Containing Metallic and Metal Oxide Nanoparticles: State of the Art and Biomedical Applications, Compounds. 3 (2023) 310–333. https://doi.org/10.3390/compounds3020023.

[11] G. Lee, B. Lee, K.-T. Kim, Mechanisms and effects of zinc oxide nanoparticle transformations on toxicity to zebrafish embryos, Environ. Sci. Nano. 8 (2021) 1690–1700. https://doi.org/10.1039/D1EN00305D.

[12] B. Brindha, M.K. Okla, S. Kokilavani, L. Sabariselvan, S.S. Al-amri, M.A. Abdel-Maksoud, G. Harini, R. Alshuwaish, W.A. Alsakkaf, S.S. Khan, Dynamic Ag-mediated electron transfer confined ZnO nanorods for boosted photocatalytic bacterial disinfection, J. Clean. Prod. 451 (2024) 141908. https://doi.org/10.1016/j.jclepro.2024.141908.

[13] A. Mikolajczyk, U. Zhdan, S. Antoniotti, A. Smolinski, K. Jagiello, P. Skurski, M. Harb, T. Puzyn, J. Polanski, Retrosynthesis from transforms to predictive sustainable chemistry and nanotechnology: a brief tutorial review, Green Chem. 25 (2023) 2971–2991. https://doi.org/10.1039/D2GC04750K.

[14] G.T. Tran, N.T.H. Nguyen, N.T.T. Nguyen, T.T.T. Nguyen, D.T.C. Nguyen, T. Van Tran, Plant extract-mediated synthesis of aluminum oxide nanoparticles for water treatment and biomedical applications: a review, Environ. Chem. Lett. 21 (2023) 2417–2439. https://doi.org/10.1007/s10311-023-01607-0.

[15] S. Sharma, K. Kumar, N. Thakur, M.S. Chauhan, Ocimum tenuiflorum leaf extract as a green mediator for the synthesis of ZnO nanocapsules inactivating bacterial pathogens, Chem. Pap. 74 (2020) 3431–3444. https://doi.org/10.1007/s11696-020-01177-3.

[16] K. Manimaran, D.H.Y. Yanto, C. Kamaraj, K. Selvaraj, S. Pandiaraj, A. M. Elgorban, S. Vignesh, H. Kim, Eco-friendly approaches of mycosynthesized copper oxide nanoparticles (CuONPs) using Pleurotus citrinopileatus mushroom extracts and their biological applications, Environ. Res. 232 (2023).

https://doi.org/10.1016/j.envres.2023.116319.

[17] S.S. Khan, S. Kokilavani, J.P. Steffy, A. Syed, A.M. Elgorban, I. Abid, L.S. Wong, Fabrication of ZnO-Cu3SnS4 NCs for enhanced visible light-induced photocatalytic degradation of carvedilol, Surfaces and Interfaces. (2024) 104875. https://doi.org/10.1016/j.surfin.2024.104875.

[18] K. Barathikannan, R. Chelliah, V. Selvakumar, F. Elahi, M. Rubab, S. Sanyal, S.-J. Yeon, D.-H. Oh, Plant-Based Metabolites and Their Uses in Nanomaterials Synthesis: An Overview, Second. Metab. Based Green Synth. Nanomater. Their Appl. (2023) 1–22. https://doi.org/10.1007/978-981-99-0927-8_1.

[19] S.S. Khan, S. Kokilavani, T.A. Alahmadi, M.J. Ansari, Enhanced visible light driven photodegradation of rifampicin and Cr(VI) reduction activity of ultra-thin ZnO nanosheets/CuCo2S4QDs: A mechanistic insights, degradation pathway and toxicity assessment, Environ. Pollut. 347 (2024) 123760. https://doi.org/10.1016/j.envpol.2024.123760.

[20] M.G. Gebremedhin, Y. Weldu, A.G. Kahsay, G. Teame, K. Adane, Extended-Spectrum β-Lactamase and Carbapenemase-Producing Gram-Negative Bacteria and Associated Factors Among Patients Suspected of Community and Hospital-Acquired Urinary Tract Infections at Ayder Comprehensive Specialized Hospital, Tigrai, Ethiopia, Infect. Drug Resist. Volume 16 (2023) 4025–4037. https://doi.org/10.2147/idr.s412350.

[21] M.M. Almoudi, A.S. Hussein, M.I. Abu Hassan, N. Mohamad Zain, A systematic review on antibacterial activity of zinc against Streptococcus mutans, Saudi Dent. J. 30 (2018) 283–291. https://doi.org/10.1016/j.sdentj.2018.06.003.

[22] F. Meyer, J. Enax, Early childhood caries: epidemiology, aetiology, Prev. 2018 (2018). https://doi.org/10.1155/2018/1415873.

[23] G. Conrads, J.J. de Soet, L. Song, K. Henne, H. Sztajer, I. Wagner-Döbler, A.P. Zeng, Comparing the cariogenic species Streptococcus sobrinus and S. mutans on whole genome level, J. Oral Microbiol. 6 (2014) 1–13. https://doi.org/10.3402/jom.v6.26189.

[24] M.K. Alshammari, M.A. Alotaibi, A.S. AlOtaibi, H.T. Alosaime, M.A. Aljuaid, B.M. Alshehri, Y.B. AlOtaibi, A.A. Alasmari, G.A. Alasmari, M.H. Mohammed, S.M.

Althobaiti, R.A. Almuhaya, T.A. Alkhoshi, A.S. Alosaimi, A.A. Alotaibi, Prevalence and Etiology of Community- and Hospital-Acquired Pneumonia in Saudi Arabia and Their Antimicrobial Susceptibility Patterns: A Systematic Review, Med. 59 (2023) 4. https://doi.org/10.3390/medicina59040760.

[25] K.U. Mahto, S. Das, Bacterial biofilm and extracellular polymeric substances in the moving bed biofilm reactor for wastewater treatment: A review, Bioresour. Technol. 345 (2022) 6. https://doi.org/10.1016/j.biortech.2021.126476.

[26] D. Dufour, V. Leung, C.M. Lévesque, Bacterial biofilm: structure, function, and antimicrobial resistance, Endod. Top. 22 (2010) 2–16. https://doi.org/10.1111/j.1601-1546.2012.00277.x.

[27] M. Krishnan, H. Subramanian, S.K. Ramachandran, A. Muthukumarasamy, D. Ramadoss, A. Mahalingam, A.J. Rathinam, H.-U. Dahms, J.-S. Hwang, Synthesis of Bimetallic BiPO4/ZnO Nanocomposite: Enhanced Photocatalytic Dye Degradation and Antibacterial Applications, Int. J. Mol. Sci. 24 (2023) 1947. https://doi.org/10.3390/ijms24031947.

[28] M.F. Ghaly, M.A. Albalawi, M.M. Bendary, A. Shahin, M.A. Shaheen, A.F. Abu Eleneen, M.M. Ghoneim, A.A. Elmaaty, M.F.M. Elrefai, S.A. Zaitone, A.I. Abousaty, Tamarindus indica Extract as a Promising Antimicrobial and Antivirulence Therapy, Antibiotics. 12 (2023) 3. https://doi.org/10.3390/antibiotics12030464.

[29] J. Wu, B. Zhang, N. Lin, J. Gao, Recent nanotechnology-based strategies for interfering with the life cycle of bacterial biofilms, Biomater. Sci. 11 (2023) 1648–1664. https://doi.org/10.1039/d2bm01783k.

[30] U. Anand, M. Carpena, M. Kowalska-Góralska, P. Garcia-Perez, K. Sunita, E. Bontempi, A. Dey, M.A. Prieto, J. Proćków, J. Simal-Gandara, Safer plant-based nanoparticles for combating antibiotic resistance in bacteria: A comprehensive review on its potential applications, recent advances, and future perspective, Sci. Total Environ. 821 (2022) 15347. https://doi.org/10.1016/j.scitotenv.2022.153472.

[31] F.J. Sutili, A. Velasquez, C.G. Pinheiro, B.M. Heinzmann, D.M. Gatlin, B. Baldisserotto, Evaluation of Ocimum americanum essential oil as an additive in red drum (Sciaenops ocellatus) diets, Fish Shellfish Immunol. 56 (2016) 155–161. https://doi.org/10.1016/j.fsi.2016.07.008.

[32] A. Luanda, A. Ripanda, Recent trend on Tetradenia riparia (Hochst.) Codd (Lamiaceae) for management of medical conditions, in: Phytomedicine Plus, Plus. org/10.1016/j.phyplu.2022.100382, 2023. https://doi.org/10.1016/j.phyplu.2022.100382.

[33] E.M. Zahran, U.R. Abdelmohsen, H.E. Khalil, S.Y. Desoukey, M.A. Fouad, M.S. Kamel, Diversity, phytochemical and medicinal potential of the genus Ocimum L. (Lamiaceae), Springer, Phytochem. Rev. Netherlands, 2020. https://doi.org/10.1007/s11101-020-09690-9.

[34] D. Shikha, P. Kashyap, Ocimum Species, in: Harvest. Food from Weeds, Wiley, 2023: pp. 183–215. https://doi.org/10.1002/9781119793007.ch6.

[35] N.A. Alamrani, Using chemically modified Ocimum tenuiflorum as an efficient and low-cost biosorbent for removing Congo red from aqueous solutions, J. Taibah Univ. Sci. 17 (2023) 2210973. https://doi.org/10.1080/16583655.2023.2210973.

[36] J.A. Kumar, T. Krithiga, S. Manigandan, S. Sathish, A.A. Renita, P. Prakash, B.S.N. Prasad, T.R.P. Kumar, M. Rajasimman, A. Hosseini-Bandegharaei, D. Prabu, S. Crispin, A focus to green synthesis of metal/metal based oxide nanoparticles: Various mechanisms and applications towards ecological approach, J. Clean. Prod. 324 (2021) 12919. https://doi.org/10.1016/j.jclepro.2021.129198.

[37] S. Asnaashari, M. Kazemnezhad, F. Masoud, Y. Javadzadeh, An overview on the anti-acne properties of herbal essential oils, J. Herb. Med. 38 (2023). https://doi.org/10.1016/j.hermed.2023.100642.

[38] P. Malav, A. Pandey, K.C. Bhatt, S. Gopala Krishnan, I.S. Bisht, Morphological variability in holy basil (Ocimum tenuiflorum L.) from India, Genet. Resour. Crop Evol. 62 (2015) 1245–1256. https://doi.org/10.1007/s10722-015-0227-5.

[39] A.K. Pandey, P. Kumar, P. Singh, N.N. Tripathi, V.K. Bajpai, Essential Oils: Sources of Antimicrobials and Food Preservatives, Front. Microbiol. 7 (2017). https://doi.org/10.3389/fmicb.2016.02161.

[40] P. Chutimanukul, P. Wanichananan, S. Janta, T. Toojinda, C.T. Darwell, K. Mosaleeyanon, The influence of different light spectra on physiological responses, antioxidant capacity and chemical compositions in two holy basil cultivars, Sci. Rep.

12 (2022) 588. https://doi.org/10.1038/s41598-021-04577-x.

[41] M. Al-Owaisi, N. Al-Hadiwi, S.A. Khan, GC-MS analysis, determination of total phenolics, flavonoid content and free radical scavenging activities of various crude extracts of Moringa peregrina (Forssk.) Fiori leaves, Asian Pac. J. Trop. Biomed. 4 (2014) 964–970. https://doi.org/10.12980/APJTB.4.201414B295.

[42] P. Singh, T.K. Roy, C. Kanupriya, P.C. Tripathi, P. Kumar, K.S. Shivashankara, Evaluation of bioactive constituents of Garcinia indica (kokum) as a potential source of hydroxycitric acid, anthocyanin, and phenolic compounds, LWT. 156 (2022) 112999. https://doi.org/10.1016/j.lwt.2021.112999.

[43] M.A. El-Shenawy, H.H. Baghdadi, L.S. El-Hosseiny, Antibacterial Activity of Plants Essential Oils Against Some Epidemiologically Relevant Food-Borne Pathogens, Open Public Health J. 8 (2015) 30–34. https://doi.org/10.2174/1874944501508010030.

[44] C. Shen, Z. Zuo, Zebrafish (Danio rerio) as an excellent vertebrate model for the development, reproductive, cardiovascular, and neural and ocular development toxicity study of hazardous chemicals, Environ. Sci. Pollut. Res. 27 (2020) 43599–43614. https://doi.org/10.1007/s11356-020-10800-5.

[45] R. Chinnasamy, K. Chinnaperumal, M. Venkatesan, K. Jogikalmat, T. Cherian, P. Willie, G. Malafaia, Eco-friendly synthesis of Ag-NPs using Endostemon viscosus (Lamiaceae): Antibacterial, antioxidant, larvicidal, photocatalytic dye degradation activity and toxicity in zebrafish embryos, Environ. Res. 218 (2023) 114946. https://doi.org/10.1016/j.envres.2022.114946.

[46] E. Haque, A.C. Ward, Zebrafish as a model to evaluate nanoparticle toxicity, Nanomaterials. 8 (2018) 561. https://doi.org/10.3390/nano8070561.

[47] J. Cueto-Escobedo, L.J. German-Ponciano, G. Guillén-Ruiz, C. Soria-Fregozo, E.V. Herrera-Huerta, Zebrafish as a Useful Tool in the Research of Natural Products With Potential Anxiolytic Effects, Front. Behav. Neurosci. 15 (2022) 5. https://doi.org/10.3389/fnbeh.2021.795285.

[48] M. MuthuKathija, M. Sheik Muhideen Badhusha, V. Rama, Green synthesis of zinc oxide nanoparticles using Pisonia Alba leaf extract and its antibacterial activity, Appl. Surf. Sci. Adv. 15 (2023) 10040. https://doi.org/10.1016/j.apsadv.2023.100400.

[49] C. Ragavendran, C. Kamaraj, K. Jothimani, A. Priyadharsan, D. Anand Kumar, D. Natarajan, G. Malafaia, Eco-friendly approach for ZnO nanoparticles synthesis and evaluation of its possible antimicrobial, larvicidal and photocatalytic applications, Sustain. Mater. Technol. 36 (2023). https://doi.org/10.1016/j.susmat.2023.e00597.

[50] T.M. Abdelghany, A.M. Al-Rajhi, R. Yahya, M.M. Bakri, A. Abboud, M. A., R. Yahya, ... & Salem, S, S. Phytofabrication Zinc Oxide Nanoparticles with Adv. Charact. Its Antioxidant, Anticancer. Antimicrob. Act. against Pathog. Microorg. 13 (2023) 417–430.

[51] N.A. Hussien, J.S. Al Malki, F.A.R. Al Harthy, A.W. Mazi, J.A.A. Al Shadadi, Sustainable Eco-Friendly Synthesis of Zinc Oxide Nanoparticles Using Banana Peel and Date Seed Extracts, Characterization, and Cytotoxicity Evaluation, Sustainability. 15 (2023) 9864. https://doi.org/10.3390/su15139864.

[52] N. Chamkouri, N. Jomehzadeh, N. Naserzadeh, Rapid biosynthesis and antibacterial activity of zinc oxide nanoparticles using fruit peel of Punica granatum L as cellulose, Curr. Res. Green Sustain. Chem. 6 (2023). https://doi.org/10.1016/j.crgsc.2023.100366.

[53] E.E. Imade, T.O. Ajiboye, A.E. Fadiji, D.C. Onwudiwe, O.O. Babalola, Green synthesis of zinc oxide nanoparticles using plantain peel extracts and the evaluation of their antibacterial activity, Sci. African. 16 (2022). https://doi.org/10.1016/j.sciaf.2022.e01152.

[54] A.W. Bauer, W.M. Kirby, J.C. Sherris, M. Turck, Antibiotic susceptibility testing by a standardized single disk method., Am. J. Clin. Pathol. 45 (1966) 493–496. https://doi.org/10.1093/ajcp/45.4_ts.493.

[55] M.T. Shaaban, M. Zayed, H.S. Salama, Antibacterial Potential of Bacterial Cellulose Impregnated with Green Synthesized Silver Nanoparticle Against S. aureus and P. aeruginosa, Curr. Microbiol. 80 (2023) 75. https://doi.org/10.1007/s00284-023-03182-7.

[56] R. Chinnasamy, K. Chinnaperumal, T. Cherian, K. Thamilchelvan, B. Govindasamy, C. Vetrivel, V. Perumal, P. Willie, P. Krutmuang, Eco-friendly phytofabrication of silver nanoparticles using aqueous extract of Aristolochia bracteolata Lam: its antioxidant potential, antibacterial activities against clinical pathogens and malarial

larvicidal effects, Biomass Convers. Biorefinery. (2023) 1–16. https://doi.org/10.1007/s13399-023-03750-8.

[57] Y. Liu, Y. Xu, Q. Song, F. Wang, L. Sun, L. Liu, X. Yang, J. Yi, Y. Bao, H. Ma, H. Huang, C. Yu, Y. Huang, Y. Wu, Y. Li, Anti-biofilm Activities From Bergenia crassifolia leaves against Streptococcus mutans, Front. Microbiol. 8 (2017) 1738. https://doi.org/10.3389/fmicb.2017.01738.

[58] G. Malafaia, A.M. de Souza, A.C. Pereira, S. Gonçalves, A.P. da Costa Araújo, R.X. Ribeiro, T.L. Rocha, Developmental toxicity in zebrafish exposed to polyethylene microplastics under static and semi-static aquatic systems, Sci. Total Environ. 700 (2020). https://doi.org/10.1016/j.scitotenv.2019.134867.

[59] N. Percie du Sert, A. Ahluwalia, S. Alam, M.T. Avey, M. Baker, W.J. Browne, A. Clark, I.C. Cuthill, U. Dirnagl, M. Emerson, P. Garner, S.T. Holgate, D.W. Howells, V. Hurst, N.A. Karp, S.E. Lazic, K. Lidster, C.J. MacCallum, M. Macleod, E.J. Pearl, O.H. Petersen, F. Rawle, P. Reynolds, K. Rooney, E.S. Sena, S.D. Silberberg, T. Steckler, H. Würbel, Reporting animal research: Explanation and elaboration for the ARRIVE guidelines 2.0, PLOS Biol. 18 (2020) e3000411. https://doi.org/10.1371/journal.pbio.3000411.

[60] C. Ragavendran, G. Balasubramani, C. Tijo, V. Manigandan, E.J. Kweka, P. Karthika, P. Sivasankar, A. Thomas, D. Natarajan, I. Nakouti, G. Malafaia, Cladophialophora bantiana metabolites are efficient in the larvicidal and ovicidal control of Aedes aegypti, and Culex quinquefasciatus and have low toxicity in zebrafish embryo, Sci. Total Environ. 852 (2022) 158502. https://doi.org/10.1016/j.scitotenv.2022.158502.

[61] K. Baskar, R. Chinnasamy, K. Pandy, M. Venkatesan, P.J. Sebastian, M. Subban, A. Thomas, E.J. Kweka, N. Devarajan, Larvicidal and histopathology effect of endophytic fungal extracts of Aspergillus tamarii against Aedes aegypti and Culex quinquefasciatus, Heliyon. 6 (2020) e05331. https://doi.org/10.1016/j.heliyon.2020.e05331.

[62] W. Mushtaq, M. Ishtiaq, M. Maqbool, M.W. Mazhar, R. Casini, A.M. Abd-ElGawad, H.O. Elansary, Green Synthesis of Zinc Oxide Nanoparticles Using Viscum album Extracts: Unveiling Bioactive Compounds, Antibacterial Potential, and Antioxidant Activities, Plants. 12 (2023) 11. https://doi.org/10.3390/plants12112130.

[63] P. Ravi, A. Elumalai, M. Chinna Eswaraiah, R. Kasarla, A review on Krishna tulsi, Ocimum tenuiflorum Linn., Int. J. Res. Ayurveda Pharm. 3 (2012) 291–293.

[64] L. Mousavi, R.M. Salleh, V. Murugaiyah, Phytochemical and bioactive compounds identification of Ocimum tenuiflorum leaves of methanol extract and its fraction with an anti-diabetic potential, Int. J. Food Prop. 21 (2018) 2390–2399. https://doi.org/10.1080/10942912.2018.1508161.

[65] C. Ragavendran, C. Kamaraj, K. Jothimani, A. Priyadharsan, D. Anand Kumar, D. Natarajan, G. Malafaia, Eco-friendly approach for ZnO nanoparticles synthesis and evaluation of its possible antimicrobial, larvicidal and photocatalytic applications, Sustain. Mater. Technol. 36 (2023) e00597. https://doi.org/10.1016/j.susmat.2023.e00597.

[66] H. Chandra, D. Patel, P. Kumari, J.S. Jangwan, S. Yadav, Phyto-mediated synthesis of zinc oxide nanoparticles of Berberis aristata: Characterization, Antioxid. Act. Antibact. Act. with Spec. Ref. to Urin. Tract Pathog. 102 (2019) 212–220.

[67] P. Basnet, T. Inakhunbi Chanu, D. Samanta, S. Chatterjee, A review on bio-synthesized zinc oxide nanoparticles using plant extracts as reductants and stabilizing agents, J. Photochem. Photobiol. B Biol. 183 (2018) 201–221. https://doi.org/10.1016/j.jphotobiol.2018.04.036.

[68] Y. Zhang, G. Qi, L. Yao, L. Huang, J. Wang, W. Gao, Effects of Metal Nanoparticles and Other Preparative Materials in the Environment on Plants: From the Perspective of Improving Secondary Metabolites, J. Agric. Food Chem. 70 (2022) 916–933. https://doi.org/10.1021/acs.jafc.1c05152.

[69] P. Kumar, S. Senthamil Selvi, M. Govindaraju, Seaweed-mediated biosynthesis of silver nanoparticles using Gracilaria corticata for its antifungal activity against Candida spp., Appl. Nanosci. 3 (2013) 495–500. https://doi.org/10.1007/s13204-012-0151-3.

[70] J.K. Park, E.J. Rupa, M.H. Arif, J.F. Li, G. Anandapadmanaban, J.P. Kang, M. Kim, J.C. Ahn, R. Akter, D.C. Yang, S.C. Kang, Synthesis of zinc oxide nanoparticles from Gynostemma pentaphyllum extracts and assessment of photocatalytic properties through malachite green dye decolorization under UV illumination-A Green Approach, Optik (Stuttg). 239 (2021) 16624. https://doi.org/10.1016/j.ijleo.2020.166249.

[71] N.K. Rajendran, B.P. George, N.N. Houreld, H. Abrahamse, Synthesis of zinc oxide nanoparticles using rubus fairholmianus root extract and their activity against pathogenic bacteria, Molecules. 26 (2021) 3029. https://doi.org/10.3390/molecules26103029.

[72] M.B. Ergönül, D. Nassouhi, M. Çelik, D. Dilbaz, D. Sazlı, S. Atasağun, Lemna trisulca L.: a novel phytoremediator for the removal of zinc oxide nanoparticles (ZnO NP) from aqueous media, Environ. Sci. Pollut. Res. 29 (2022) 90852–90867. https://doi.org/10.1007/s11356-022-22112-x.

[73] H.K. Narendra Kumar, N. Chandra Mohana, B.R. Nuthan, K.P. Ramesha, D. Rakshith, N. Geetha, S. Satish, Phyto-mediated synthesis of zinc oxide nanoparticles using aqueous plant extract of Ocimum americanum and evaluation of its bioactivity, SN Appl. Sci. 1 (2019) 1–9. https://doi.org/10.1007/s42452-019-0671-5.

[74] B. Almutairi, G. Albahser, R. Almeer, N.M. Alyami, H. Almukhlafi, K.N. Yaseen, S. Alkahtani, S. Alarifi, M. Saxena, Investigation of Cytotoxicity Apoptotic and Inflammatory Responses of Biosynthesized Zinc Oxide Nanoparticles from Ocimum sanctum Linn in Human Skin Keratinocyte (Hacat) and Human Lung Epithelial (A549) Cells, Oxid. Med. Cell. Longev. 2020 (2020). https://doi.org/10.1155/2020/1835475.

[75] D.H. Abdelkader, W.A. Negm, E. Elekhnawy, D. Eliwa, B.N. Aldosari, A.S. Almurshedi, Zinc Oxide Nanoparticles as Potential Delivery Carrier: Green Synthesis by Aspergillus niger Endophytic Fungus, Characterization, and In Vitro/In Vivo Antibacterial Activity, Pharmaceuticals. 15 (2022) 1057. https://doi.org/10.3390/ph15091057.

[76] Y.H.I. Mohammed, S. Alghamdi, B. Jabbar, D. Marghani, S. Beigh, A.S. Abouzied, N.E. Khalifa, W.M.A. Khojali, B. Huwaimel, D.H.M. Alkhalifah, W.N. Hozzein, Green Synthesis of Zinc Oxide Nanoparticles Using Cymbopogon citratus Extract and Its Antibacterial Activity, ACS Omega. 8 (2023) 32027–32042. https://doi.org/10.1021/acsomega.3c03908.

[77] A. Jayachandran, A. T.R., A.S. Nair, Green synthesis and characterization of zinc oxide nanoparticles using Cayratia pedata leaf extract, Biochem. Biophys. Reports. 26 (2021) 5. https://doi.org/10.1016/j.bbrep.2021.100995.

881 [78] P. Srinivasan, A. Sudha, J. Jeyaraman, Green synthesis of silver nanoparticles using
882 Lippia nodiflora aerial extract and evaluation of their antioxidant, antibacterial and
883 cytotoxic effects, Resour. Technol. 3 (2017) 506–515.
884 https://doi.org/10.18799/24056529/2017/4/167.

885 [79] R.E. Mfon, S.R. Hall, A. Sarua, Effect of Ocimum gratissimum plant leaf extract
886 concentration and annealing temperature on the structure and optical properties of
887 synthesized zinc oxide nanoparticles, Educ. J. Sci. Math. Technol. 7 (2020) 1–13.
888 https://doi.org/10.37134/ejsmt.vol7.1.1.2020.

889 [80] S. Singh, S. Datta, K.B. Narayanan, K.N. Rajnish, Bacterial exo-polysaccharides in
890 biofilms: role in antimicrobial resistance and treatments, J. Genet. Eng. Biotechnol. 19
891 (2021) 140. https://doi.org/10.1186/s43141-021-00242-y.

892 [81] H. Kamyab, S. Chelliapan, G. Hayder, M. Yusuf, M.M. Taheri, S. Rezania, M. Hasan,
893 K.K. Yadav, M. Khorami, M. Farajnezhad, J. Nouri, Exploring the potential of metal
894 and metal oxide nanomaterials for sustainable water and wastewater treatment: A
895 review of their antimicrobial properties, Chemosphere. 335 (2023).
896 https://doi.org/10.1016/j.chemosphere.2023.139103.

897 [82] J. Ma, K. Li, S. Gu, Selective strategies for antibacterial regulation of nanomaterials,
898 RSC Adv. 12 (2022) 4852–4864. https://doi.org/10.1039/D1RA08996J.

899 [83] Sachin, Jaishree, N. Singh, R. Singh, K. Shah, B.K. Pramanik, Green synthesis of zinc
900 oxide nanoparticles using lychee peel and its application in anti-bacterial properties
901 and CR dye removal from wastewater, Chemosphere. 327 (2023) 7.
902 https://doi.org/10.1016/j.chemosphere.2023.138497.

903 [84] A. Fouda, E. Saied, A.M. Eid, F. Kouadri, A.M. Alemam, M.F. Hamza, M. Alharbi, A.
904 Elkelish, S.E.D. Hassan, Green Synthesis of Zinc Oxide Nanoparticles Using an
905 Aqueous Extract of Punica granatum for Antimicrobial and Catalytic Activity, J.
906 Funct. Biomater. 14 (2023) 4. https://doi.org/10.3390/jfb14040205.

907 [85] X. Yang, X. Cao, C. Chen, L. Liao, S. Yuan, S. Huang, Green Synthesis of Zinc Oxide
908 Nanoparticles Using Aqueous Extracts of Hibiscus cannabinus L.: Wastewater
909 Purification and Antibacterial Activity, Separations. 10 (2023) 466.
910 https://doi.org/10.3390/separations10090466.

[86] Y. Li, J. Li, M. Li, J. Sun, X. Shang, Y. Ma, Biological mechanism of <scp>ZnO</scp> nanomaterials, J. Appl. Toxicol. (2023). https://doi.org/10.1002/jat.4522.

[87] A. Laganà, G. Visalli, F. Corpina, M. Ferlazzo, A.D.I. Pietro, A. Facciolà, Antibacterial activity of nanoparticles and nanomaterials: a possible weapon in the fight against healthcare-associated infections, Eur. Rev. Med. Pharmacol. Sci. 27 (2023) 3645–3663. https://doi.org/10.26355/eurrev_202304_32151.

[88] J. Xie, H. Li, T. Zhang, B. Song, X. Wang, Z. Gu, Recent Advances in ZnO Nanomaterial-Mediated Biological Applications and Action Mechanisms, Nanomaterials. 13 (2023) 1500. https://doi.org/10.3390/nano13091500.

[89] R.M. Al-Mosawi, R.M. Al-Badr, The Study Effects of Dental Composite Resin as Antibacterial Agent Which Contain Nanoparticles of Zinc Oxide on the Bacteria Associated with Oral Infection, IOSR J. Dent. Med. Sci. 16 (2017) 49–55. https://doi.org/10.9790/0853-1601014955.

[90] R. Krishnamoorthy, J. Athinarayanan, V.S. Periyasamy, M.A. Alshuniaber, G. Alshammari, M.J. Hakeem, M.A. Ahmed, A.A. Alshatwi, Antibacterial Mechanisms of Zinc Oxide Nanoparticle against Bacterial Food Pathogens Resistant to Beta-Lactam Antibiotics, Molecules. 27 (2022) 8. https://doi.org/10.3390/molecules27082489.

[91] C.R. Mendes, G. Dilarri, C.F. Forsan, V. de M.R. Sapata, P.R.M. Lopes, P.B. de Moraes, R.N. Montagnolli, H. Ferreira, E.D. Bidoia, Antibacterial action and target mechanisms of zinc oxide nanoparticles against bacterial pathogens, Sci. Rep. 12 (2022) 1. https://doi.org/10.1038/s41598-022-06657-y.

[92] Happy Agarwal, S. Menon, S. Venkat Kumar, S. Rajeshkumar, Mechanistic study on antibacterial action of zinc oxide nanoparticles synthesized using green route, Chem. Biol. Interact. 286 (2018) 60–70. https://doi.org/10.1016/j.cbi.2018.03.008.

[93] U.L. Ifeanyichukwu, O.E. Fayemi, C.N. Ateba, Green Synthesis of Zinc Oxide Nanoparticles from Pomegranate (Punica granatum) Extracts and Characterization of Their Antibacterial Activity, Molecules. 25 (2020) 4521. https://doi.org/10.3390/molecules25194521.

[94] S. Hayat, A. Ashraf, M. Zubair, B. Aslam, M.H. Siddique, M. Khurshid, M. Saqalein, A.M. Khan, A. Almatroudi, Z. Naeem, S. Muzammil, Biofabrication of ZnO nanoparticles using Acacia arabica leaf extract and their antibiofilm and antioxidant potential against foodborne pathogens, PLoS One. 17 (2022) e0259190. https://doi.org/10.1371/journal.pone.0259190.

[95] L. Pang, H. Lin, F. Yang, D. Deng, Editorial: Mechanisms of biofilm development and antibiofilm strategies, Front. Microbiol. 14 (2023) 1098. https://doi.org/10.3389/fmicb.2023.1190611.

[96] D. Windaryanti, C.S. Gabriel, I.W. Hidayat, A. Zainuddin, H.D.A. Dharsono, M.H. Satari, D. Kurnia, The Potential of 24-Propylcholestrol as Antibacterial Oral Bacteria of Enterococcus faecalis ATCC 29212 and Inhibitor Biofilms Formation: in vitro and in silico Study, Adv. Appl. Bioinforma. Chem. 15 (2022) 99–111. https://doi.org/10.2147/AABC.S372337.

[97] M. Fernandes, N. González-Ballesteros, A. da Costa, R. Machado, A.C. Gomes, M.C. Rodríguez-Argüelles, Antimicrobial and anti-biofilm activity of silver nanoparticles biosynthesized with Cystoseira algae extracts, JBIC J. Biol. Inorg. Chem. 28 (2023) 439–450. https://doi.org/10.1007/s00775-023-01999-y.

[98] V. Unni, P. Abishad, P.R. Arya, B. Mohan, S. Juliet, L. John, P. Nambiar, V.K. Vinod, A. Karthikeyan, N.V. Kurkure, S.B. Barbuddhe, D.B. Rawool, J. Vergis, Eco-Friendly One Pot Synthesis of Zinc Oxide Nanoparticles Using Catkin Extract of Piper longum: In Vitro Antibacterial, Antioxidant and Antibiofilm Potential against Multi Drug Resistant Enteroaggregative E. coli, in: 2nd Int. Electron. Conf. Biomed., MDPI, Basel Switzerland, 2023: p. 14. https://doi.org/10.3390/ECB2023-14269.

[99] A. Agrawal, R. Sharma, A. Sharma, K.C. Gurjar, S. Kumar, S. Chatterjee, H. Pandey, K. Awasthi, A. Awasthi, Antibacterial and antibiofilm efficacy of green synthesized ZnO nanoparticles using Saraca asoca leaves, Environ. Sci. Pollut. Res. (2023) 1–10. https://doi.org/10.1007/s11356-023-28524-7.

[100] M. Altaf, M.T. Zeyad, M.A. Hashmi, S. Manoharadas, S.A. Hussain, M.S. Ali Abuhasil, M.A.M. Almuzaini, Effective inhibition and eradication of pathogenic biofilms by titanium dioxide nanoparticles synthesized using Carum copticum extract, RSC Adv. 11 (2021) 19248–19257. https://doi.org/10.1039/D1RA02876F.

[101] N. Rani, S. Rani, H. Patel, Bhavna, S. Yadav, M. Saini, S. Rawat, K. Saini, Characterization and investigation of antioxidant and antimicrobial activity of zinc oxide nanoparticles prepared using leaves extract of Nyctanthes arbor-tristis, Inorg. Chem. Commun. 150 (2023) 6. https://doi.org/10.1016/j.inoche.2023.110516.

[102] A. Abdelghafar, N. Yousef, M. Askoura, Zinc oxide nanoparticles reduce biofilm formation, synergize antibiotics action and attenuate Staphylococcus aureus virulence in host; an important message to clinicians, BMC Microbiol. 22 (2022) 244. https://doi.org/10.1186/s12866-022-02658-z.

[103] U. Vicario-Parés, L. Castañaga, J.M. Lacave, M. Oron, P. Reip, D. Berhanu, E. Valsami-Jones, M.P. Cajaraville, A. Orbea, Comparative toxicity of metal oxide nanoparticles (CuO, ZnO and TiO2) to developing zebrafish embryos, J. Nanoparticle Res. 16 (2014) 2550. https://doi.org/10.1007/s11051-014-2550-8.

[104] H. Xie, M. Li, Y. Kang, J. Zhang, C. Zhao, Zebrafish: an important model for understanding scoliosis, Cell. Mol. Life Sci. 79 (2022) 506. https://doi.org/10.1007/s00018-022-04534-5.

[105] J.S. Choi, R.-O. Kim, S. Yoon, W.-K. Kim, Developmental Toxicity of Zinc Oxide Nanoparticles to Zebrafish (Danio rerio): A Transcriptomic Analysis, PLoS One. 11 (2016) e0160763. https://doi.org/10.1371/journal.pone.0160763.

[106] W. Bai, Z. Zhang, W. Tian, X. He, Y. Ma, Y. Zhao, Z. Chai, Toxicity of zinc oxide nanoparticles to zebrafish embryo: A physicochemical study of toxicity mechanism, J. Nanoparticle Res. 12 (2010) 1645–1654. https://doi.org/10.1007/s11051-009-9740-9.

[107] C. Bai, M. Tang, Toxicological study of metal and metal oxide nanoparticles in zebrafish, J. Appl. Toxicol. 40 (2020) 37–63. https://doi.org/10.1002/jat.3910.

[108] Y.-L. Lee, Y.-S. Shih, Z.-Y. Chen, F.-Y. Cheng, J.-Y. Lu, Y.-H. Wu, Y.-J. Wang, Toxic Effects and Mechanisms of Silver and Zinc Oxide Nanoparticles on Zebrafish Embryos in Aquatic Ecosystems, Nanomaterials. 12 (2022) 717. https://doi.org/10.3390/nano12040717.

1002

1003

1004

1005